

Geometry-Inspired Top- k Adversarial Perturbations

Nurislam Tursynbek,¹ Aleksandr Petiushko,^{2,3} Ivan Oseledets¹

¹Skolkovo Institute of Science and Technology, ²Huawei MRC, ³Lomonosov Moscow State University

nurislam.tursynbek@gmail.com, petushko.alexander1@huawei.com, i.oseledets@skolecch.ru

Abstract

Deep learning models are vulnerable to adversarial examples, which endangers their usage in real-world applications. The main target of existing adversarial perturbations is primarily limited to change the correct Top-1 predicted class by the incorrect one, which does not intend changing the Top- k prediction. However, in many real-world scenarios, especially dealing with digital images, Top- k predictions are more important. In this work, we propose a simple yet effective geometry-inspired method of computing Top- k adversarial examples for any k . We evaluate its effectiveness and efficiency by comparing it with other adversarial example crafting techniques. Moreover, based on this method, we propose Top- k Universal Adversarial Perturbations, image-agnostic tiny perturbations that cause true class to be absent among the Top- k prediction for most inputs in the dataset. We experimentally show that our approach outperforms baseline methods and even improves existing techniques of generating Universal Adversarial Perturbations.

1. Introduction

Besides significantly revolutionizing wide range of tasks, Deep Neural Networks (DNNs) are intriguingly found to be brittle to imperceptibly perturbed inputs, also known as adversarial examples [35, 14, 8]. These malicious well-designed perturbations are carefully crafted in order to cause neural networks to make a mistake. They may attempt to target a specific wrong class to be a prediction (targeted attack), or to yield a class any different from the true one (untargeted attack). Advances of adversarial perturbations found potential vulnerabilities of practical safety-critical applications of DNNs in self-driving cars [12, 15], speech recognition systems [2, 9], face identification [33, 21]. Moreover, modern defenses to adversarial attacks are found to be ineffective [3, 36]. These security issues compromise people’s confidence in DNNs, and thus it is necessary and crucial to investigate and study different types of adversarial attacks on deep learning models.

Recently, DeepFool [27] was proposed as an efficient approach of constructing small adversarial noise, which analytically finds a perturbation in the direction towards classifier’s closest decision boundary, that is computed with linear approximation using Taylor expansion. Based on the fact that DeepFool quickly finds the necessary perturbation of small norm, in [26] it was discovered a way of constructing small input-agnostic universal adversarial perturbations (UAPs), mere addition of which cause neural networks to make mistakes on majority of inputs, even on unseen images. The existence and transferability between different models of such perturbations show the threats of DNNs deployment in the real-world scenarios, as adversaries can straightforwardly compute and exploit them in a malicious manner.

Although few adversarial attacks are found to be physically realizable [7, 4], the vast majority of adversarial perturbations are pixel-wise and tested on digital images. In many real-world applications of DNNs, dealing with digital images, such as computer vision cloud APIs (Google Cloud Vision¹, Amazon Rekognition², IBM Watson Visual Recognition³, Microsoft Azure Computer Vision⁴, Clarifai⁵), recommendation systems, web search engines, Top- k prediction is more important and meaningful, since a user usually gets Top- k classes corresponding to a particular request, and some of them are usually difficult to discriminate. However, the existing techniques of computing adversarial examples (including UAPs) mainly target fooling the Top-1 prediction of DNNs, sometimes even just swapping classes from the Top-2 prediction, which still makes the true class to be present among Top- k prediction. We attempt to fill this gap and geometrically extend DeepFool [27] and UAP [26] to the case of a Top- k adversary. Visual illustration of a Top- k UAP is shown in Fig. 1.

¹<https://cloud.google.com/vision>

²<https://aws.amazon.com/rekognition/>

³<https://cloud.ibm.com/catalog/services/visual-recognition>

⁴<https://azure.microsoft.com/en-us/services/cognitive-services/computer-vision/>

⁵<https://www.clarifai.com/>

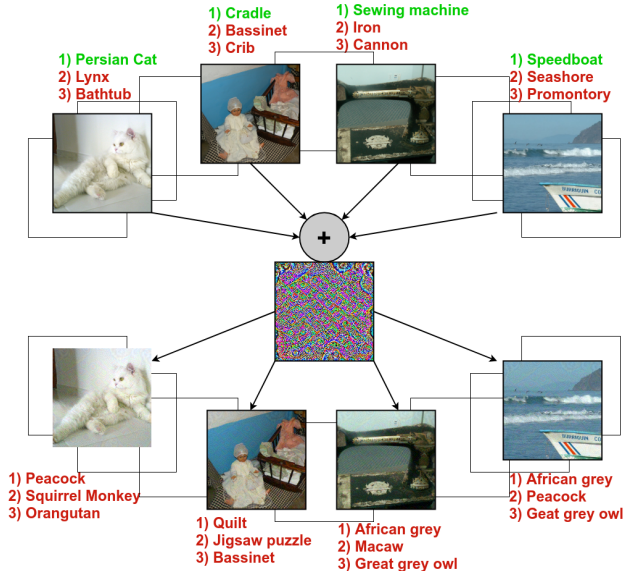


Figure 1. Visual illustration of Top- k Universal Adversarial Perturbation calculated for VGG-16 neural network [34]. A mere addition of a single small (here, ℓ_∞ -bound is 10) perturbation makes true classes of initial images to be outside of Top- k (here, $k = 3$) prediction of perturbed images for high percentage of the unseen images.

Main contributions of this paper are following:

- We propose $kFool$ - a geometrically-motivated approach to efficiently compute a Top- k adversarial perturbation to an image that makes the true class to be absent among the Top- k prediction. Inspired by the idea of DeepFool [27], we linearly approximate decision boundaries using Taylor expansion and find the so-called "bisection" direction that simultaneously push data point maximally closer to classifier's k nearest decision boundaries.
- We show effectiveness and efficiency of $kFool$, by demonstrating that it is possible to construct a Top- k adversarial perturbation of a small magnitude, bounded either in ℓ_2 or ℓ_∞ , and compare it to popular existing Top-1 adversarial perturbations crafting techniques.
- We propose *Top-k Universal Adversarial Perturbations (kUAPs)*, based on $kFool$, that extends the idea of UAPs, which was based on DeepFool, to Top- k prediction.
- We experimentally show that $kUAPs$ outperform baseline methods and even improve existing techniques of generating UAPs on standard ILSVRC2012 validation dataset.

2. Background

Here, we describe preliminaries of adversarial examples to introduce our method. Given an input image $\mathbf{x} \in \mathcal{R}^m$ and a neural network classifier $F : \mathcal{R}^m \rightarrow \mathcal{R}^C$ for C classes, the adversarial perturbation (which we call *Top-1 adversarial perturbation*) for an input \mathbf{x} , as found in [35], is a noise $\mathbf{v} \in \mathcal{R}^m$, such that the norm of the perturbation is small, $\|\mathbf{v}\| \leq \varepsilon$, and the perturbed image is misclassified, or formally:

$$\arg \max F(\mathbf{x}) \neq \arg \max F(\mathbf{x} + \mathbf{v}). \quad (1)$$

Similarly, we also introduce *Top-k adversarial perturbation*, i.e. the original class is outside of the largest k components of $F(\mathbf{x} + \mathbf{v})$:

$$\arg \max F(\mathbf{x}) \notin \arg \text{sort } F(\mathbf{x} + \mathbf{v})[:k] \quad (2)$$

The new input $\mathbf{x} + \mathbf{v}$ should satisfy constraints on pixel values. The task is usually to find an *optimal perturbation*: the perturbation that satisfies (1) or (2) and has minimal norm.

The classical work of [14] proposed a single-step way to craft an adversarial perturbation with small ℓ_∞ -bound value of ε for an input \mathbf{x} with a true label y , called *Fast Gradient Sign Method (FGSM)*, using gradient of a loss function \mathcal{L} (typically, cross-entropy) between the prediction $F(\mathbf{x})$ and the label y :

$$\mathbf{x}_{adv} = \mathbf{x} + \varepsilon \text{sign}(\nabla_{\mathbf{x}} \mathcal{L}(F(\mathbf{x}), y)), \quad (3)$$

The iterative version of FGSM is called PGD [22]. It finds a perturbation of small norm but requires a significant amount of time. Our work is built upon the *DeepFool* [27], where a geometry-inspired fast way of calculation of an adversarial perturbation in the approximate direction to the nearest boundary was presented. Suppose, we have a linear binary classifier $f(\mathbf{x}) = \mathbf{w}^T \mathbf{x} + b$ with separating plane $f(\mathbf{x}) = 0$ and the given input point \mathbf{x}_0 . The optimal (small norm) adversarial perturbation is the distance to the separating plane $\mathbf{w}^T \mathbf{x} + b = 0$ of the binary classifier. This distance is computed as:

$$\mathbf{r} = -\frac{|f(\mathbf{x}_0)|}{\|\mathbf{w}\|_2} \mathbf{w}, \quad (4)$$

and its magnitude is $d = \|\mathbf{r}\|_2 = \frac{|f(\mathbf{x}_0)|}{\|\mathbf{w}\|_2}$. Equation (4) can be extended to an arbitrary binary deep classifier and also to the multi-class case. For an arbitrary differentiable classifier, the first-order Taylor expansion allows to approximate as:

$$\mathbf{w} \approx \nabla_{\mathbf{x}} f, \quad (5)$$

and to generalize to the multi-class case, one can use the "one-vs-all" classification scheme.

Specifically, for an input \mathbf{x}_0 and i -th decision boundary, the corresponding function is $f_i(\mathbf{x}) = F_{true}(\mathbf{x}) - F_i(\mathbf{x})$ and $\mathbf{w}_i = \nabla_{\mathbf{x}} F_{true}(\mathbf{x}) - \nabla_{\mathbf{x}} F_i(\mathbf{x})$, where F_i is the output logit of a neural network corresponding to the class i . Thus, the ℓ_2 -minimal perturbation \mathbf{r} needed to fool this linearly approximated classifier for \mathbf{x}_0 can be computed as:

$$c = \arg \min_{i \neq true} \frac{|F_i(\mathbf{x}_0) - F_{true}(\mathbf{x}_0)|}{\|\nabla_{\mathbf{x}} F_i(\mathbf{x}_0) - \nabla_{\mathbf{x}} F_{true}(\mathbf{x}_0)\|_2} \quad (6)$$

$$\mathbf{r} = \frac{|F_c(\mathbf{x}_0) - F_{true}(\mathbf{x}_0)|}{\|\nabla_{\mathbf{x}} F_c(\mathbf{x}_0) - \nabla_{\mathbf{x}} F_{true}(\mathbf{x}_0)\|_2^2} \times (\nabla_{\mathbf{x}} F_c(\mathbf{x}_0) - \nabla_{\mathbf{x}} F_{true}(\mathbf{x}_0)) \quad (7)$$

The ℓ_∞ -minimal perturbation to the nearest boundary is:

$$c = \arg \min_{i \neq true} \frac{|F_i(\mathbf{x}_0) - F_{true}(\mathbf{x}_0)|}{\|\nabla_{\mathbf{x}} F_i(\mathbf{x}_0) - \nabla_{\mathbf{x}} F_{true}(\mathbf{x}_0)\|_1} \quad (8)$$

$$\mathbf{r} = \frac{|F_c(\mathbf{x}_0) - F_{true}(\mathbf{x}_0)|}{\|\nabla_{\mathbf{x}} F_c(\mathbf{x}_0) - \nabla_{\mathbf{x}} F_{true}(\mathbf{x}_0)\|_1} \text{sgn}(\nabla_{\mathbf{x}} F_c(\mathbf{x}_0) - \nabla_{\mathbf{x}} F_{true}(\mathbf{x}_0)) \quad (9)$$

Since the first-order Taylor expansion is linear approximation, it may deviate from the actual decision boundaries of the classifier. Therefore, the procedure should be repeated in an iterative manner: the original image is perturbed, then a new perturbation vector for the perturbed image is computed and so on. However, only few iterations are needed for DeepFool algorithm to quickly reach an incorrect class, finding an efficient Top-1 adversarial perturbation.

3. k Fool

Here, we describe our proposed method k Fool - an efficient way of finding Top- k adversarial perturbation, based on geometric properties between k nearest boundaries.

DeepFool iterations quickly reach the incorrect class, and swaps classes from Top-2 prediction. However, our target is different: we need to construct the Top- k perturbation, i.e. perturb the initial image such that the true class is not only outside the Top-1 prediction, but it is outside the Top- k prediction. DeepFool may not give such a result, however, by considering k decision boundaries we can construct such a perturbation in the same computational cost as the DeepFool.

For simplicity reasons, we first consider $k = 2$ closest linearized decision boundaries (see Fig. 2). Originally, DeepFool directions (\mathbf{r}_1 or \mathbf{r}_2 , which are opposite to corresponding normal vectors \mathbf{w}_1 and \mathbf{w}_2 of decision boundaries) bring data point closer to one boundary, and unfortunately might move away data point from another. Thus, to attack Top- k prediction, the adversary needs to find a direction which brings the data point closer to all k (here, $k = 2$) boundaries (green region in Fig. 2).

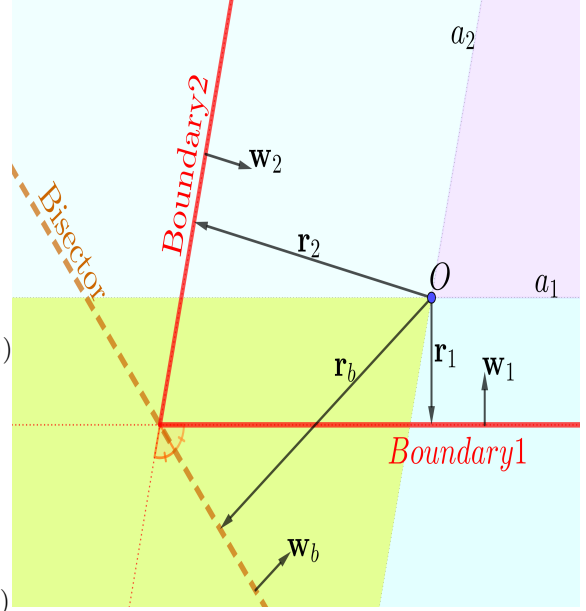


Figure 2. The geometric illustration of a single step of k Fool for $k = 2$. The data point O is inside the true class region surrounded by $k = 2$ closest linear decision boundaries to incorrect classes. a_1 and a_2 are auxiliary planes passing through O , parallel to the boundaries. Perturbation in the purple region pushes away point O from both boundaries. Perturbation in the blue regions brings closer the point O to one boundary, but pushes away from another (DeepFool). Perturbation in the green region brings the point O closer to both boundaries (k Fool).

The magnitudes of distances to decision boundaries can be computed using (4) and $f_i(\mathbf{x}) = F_{true}(\mathbf{x}) - F_i(\mathbf{x}) > 0$, which gives:

$$\|\mathbf{r}_i\|_2 = \frac{f_i(\mathbf{x})}{\|\mathbf{w}_i\|_2} = \frac{\mathbf{w}_i^T \mathbf{x} + b_i}{\|\mathbf{w}_i\|_2} \quad (10)$$

To find the most optimal direction of perturbation that maximally reduces the sum of distances to k closest boundaries and simultaneously bring the data point closer to all of them, we first solve following problem:

$$\mathbf{w}_b = \arg \max_{\mathbf{x}} \sum_{i=1}^k \|\mathbf{r}_i\|_2 = \frac{\partial \sum_{i=1}^k \|\mathbf{r}_i\|_2}{\partial \mathbf{x}} = \sum_{i=1}^k \frac{\mathbf{w}_i}{\|\mathbf{w}_i\|_2} \quad (11)$$

Then, the direction of Top- k perturbation \mathbf{r}_b is exactly opposite to \mathbf{w}_b . As seen in the Figure 2, this direction is also perpendicular to the bisector line of the exterior angle between the boundaries. As we found the direction of the perturbation, next we need the magnitude of \mathbf{r}_b . Following the analogy from Equation (4), to compute the magnitude of the perturbation \mathbf{r}_b , we assume the Top- k perturbation is the distance to the bisector line. Then, we need to calculate

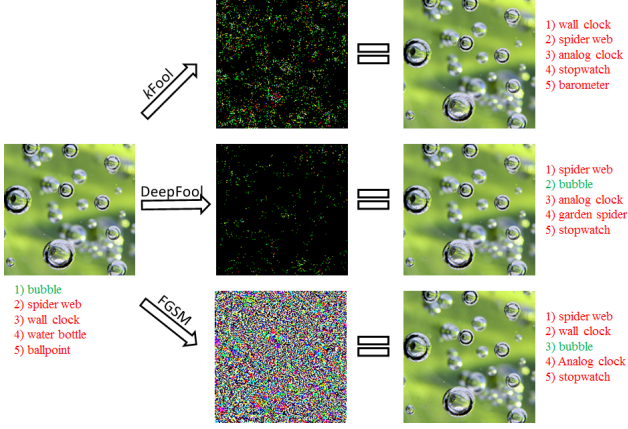


Figure 3. Examples of k Fool ($k = 5$), DeepFool [27] and FGSM [14] adversarial perturbations. For the k Fool-perturbed image, true class is absent among Top- k predictions, while for the image perturbed by DeepFool and FGSM true class is present among Top- k prediction, which shows the superiority of k Fool. Moreover, visually k Fool produces perturbation even smaller than FGSM and comparable to DeepFool, however latter two use more simple task statement.

$f_b = \mathbf{w}_b^T \mathbf{x} + b_b$. To find b_b we assume there is an "intersection" point \mathbf{x}^* , where $0 = f_1(\mathbf{x}^*) = f_2(\mathbf{x}^*) = \dots = f_i(\mathbf{x}^*) = \dots$. Then $f_b(\mathbf{x}^*)$ is also equal to 0, meaning $f_b(\mathbf{x}^*) = \mathbf{w}_b^T \mathbf{x}^* + b_b = 0$. Using this:

$$b_b = -\mathbf{w}_b^T \mathbf{x}^* = -\sum_{i=1}^k \frac{\mathbf{w}_i^T \mathbf{x}^*}{\|\mathbf{w}_i\|_2} = \sum_{i=1}^k \frac{b_i}{\|\mathbf{w}_i\|_2}. \quad (12)$$

Then:

$$f_b(\mathbf{x}) = \mathbf{w}_b^T \mathbf{x} + b_b = \sum_{i=1}^k \frac{f_i(x)}{\|\mathbf{w}_i\|_2} \quad (13)$$

Then, using p as an index array of sorted logits $F(\mathbf{x})$ in descending order, setting $f_i = F_{p[i]}(\mathbf{x}) - F_{true}(\mathbf{x})$ and $\mathbf{w}_i = \nabla_{\mathbf{x}} F_{p[i]}(\mathbf{x}) - \nabla_{\mathbf{x}} F_{true}(\mathbf{x})$, we have:

$$\mathbf{r}_b = -\frac{|f_b(\mathbf{x}_0)|}{\|\mathbf{w}_b\|_2} \mathbf{w}_b = \frac{\sum_{i=1}^k \frac{f_i(x)}{\|\mathbf{w}_i\|_2}}{\left\| \sum_{i=1}^k \frac{\mathbf{w}_i}{\|\mathbf{w}_i\|_2} \right\|_2} \sum_{i=1}^k \frac{\mathbf{w}_i}{\|\mathbf{w}_i\|_2} \quad (14)$$

Similarly to DeepFool, it might be not enough to add a perturbation only once to satisfy the goal (true class is absent among largest k predictions), thus we do a few iterations for that (see Algorithm 1).

Extension of (14) to ℓ_∞ is straightforward, as we follow DeepFool's extension in Eq. (8) and Eq. (9):

Algorithm 1 k Fool

INPUT: k , Image \mathbf{x} , its label: $true$, classifier F with logits $\{F_1, \dots, F_C\}$

```

1:  $p \leftarrow \arg \text{sort}(F(\mathbf{x}))$  ▷ In descending order
2:  $\mathbf{r} \leftarrow \mathbf{0}$ 
3: while  $true$  in  $p[:k]$  do
4:    $\mathbf{w}_b \leftarrow \mathbf{0}$ 
5:    $f_b \leftarrow 0$ 
6:   for  $i = 1$  to  $k + 1$  do:
7:      $\mathbf{w}_b \leftarrow \mathbf{w}_b + \frac{\nabla_{\mathbf{x}} F_{p[i]}(\mathbf{x}) - \nabla_{\mathbf{x}} F_{true}(\mathbf{x})}{\|\nabla_{\mathbf{x}} F_{p[i]}(\mathbf{x}) - \nabla_{\mathbf{x}} F_{true}(\mathbf{x})\|_2}$ 
8:      $f_b \leftarrow f_b + \frac{F_{p[i]}(\mathbf{x}) - F_{true}(\mathbf{x})}{\|\nabla_{\mathbf{x}} F_{p[i]}(\mathbf{x}) - \nabla_{\mathbf{x}} F_{true}(\mathbf{x})\|_2}$ 
9:   end for
10:   $\mathbf{r} \leftarrow \mathbf{r} + \frac{|f_b|}{\|\mathbf{w}_b\|_2} \mathbf{w}_b$ 
11:   $p \leftarrow \arg \text{sort}(F(\mathbf{x} + \mathbf{r}))$  ▷ In descending order
12: end while

```

OUTPUT: Top- k Adversarial Perturbation \mathbf{r}

$$\mathbf{r}_b = -\frac{|f_b(\mathbf{x}_0)|}{\|\mathbf{w}_b\|_1} \text{sign}(\mathbf{w}_b) = \frac{\sum_{i=1}^k \frac{f_i(x)}{\|\mathbf{w}_i\|_2}}{\left\| \sum_{i=1}^k \frac{\mathbf{w}_i}{\|\mathbf{w}_i\|_2} \right\|_1} \text{sign} \left(\sum_{i=1}^k \frac{\mathbf{w}_i}{\|\mathbf{w}_i\|_2} \right) \quad (15)$$

Comparative illustration of k Fool perturbation is shown in Fig. 3. The quantitative experimental comparison is presented in the Section 5.1.

4. k UAP

UAP [26] solves the problem in the Equation (2) for most of images simultaneously. To find such a universal direction that fools the majority of images, DeepFool [27] algorithm was applied in an iterative manner over the dataset of images, as it finds a small Top-1 adversarial perturbation efficiently. To satisfy the constraint of smallness of noise, at each time a new perturbation is projected to the ℓ_p -ball, suitable for that.

Inspired by the existence of such directions, we propose Top- k UAPs (k UAPs). Following [26], we apply the k Fool direction iteratively to the dataset, to find a perturbation, mere addition of which to most of natural images makes their true classes to be outside of Top- k predictions. Formally, the goal of k UAP is to find a noise \mathbf{v} that satisfies two following conditions:

1. $\mathbb{P}_{\mathbf{x} \sim \mu} [\arg \max(F(\mathbf{x})) \notin \arg \text{sort}(F(\mathbf{x} + \mathbf{v}))[:k]] \geq \zeta$
2. $\|\mathbf{v}\|_p \leq \varepsilon$

In the above criteria, μ is the distribution of natural images from which \mathbf{x} is drawn, and this distribution varied over

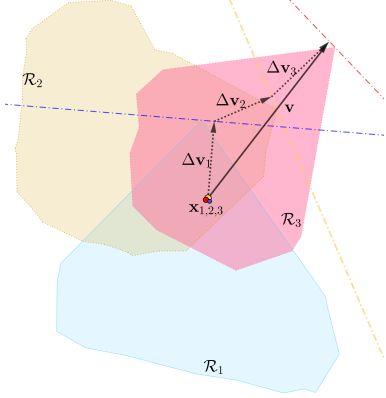


Figure 4. Schematic illustration of k UAP procedure. Data points x_1, x_2, x_3 from different classes (with decision regions $\mathcal{R}_1, \mathcal{R}_2, \mathcal{R}_3$) are super-imposed. Then, iteratively k Fool is applied that sends points in the direction of the bisector of the exterior angle between k nearest boundaries.

the dataset. Adversarial strength ε is the maximum ℓ_p norm of the noise \mathbf{v} . The $\text{argsort}(F_i(\cdot))[k]$ operator gets the first k indices of sorted output logits F_i (i.e. the Top- k prediction). The parameter ζ quantifies the desired fooling rate — i.e. the fraction of images Top- k prediction of which should be fooled.

Algorithm. Given a dataset $X = \{\mathbf{x}_1, \dots, \mathbf{x}_N\} \sim \mu$, our proposed algorithm k UAP searches for a direction $\|\mathbf{v}\|_p \leq \varepsilon$, the addition of which to $(1-\delta)$ fraction of images makes their true label ($\arg \max_i (F_i(\mathbf{x}))$) to be outside of Top- k prediction ($\arg \text{sort}(F_i(\mathbf{x}+\mathbf{v}))[k]$). Following [26], we propose to apply k Fool (which finds the normal vector to the “bisector of an exterior angle between the nearest k decision boundaries” (see Algorithm 1)) iteratively over data samples from X . The illustrative schematic of the procedure is demonstrated in Fig. 4. First, all images are super-imposed into one starting point and \mathbf{v} is initialized as a zero vector. At each iteration i , Algorithm finds k Fool direction $\Delta \mathbf{v}_i$ for a given data point $\mathbf{x}_i + \mathbf{v}$, which fools the Top- k prediction for the current image \mathbf{x}_i , and updates the current universal perturbation \mathbf{v} simply by $\mathbf{v} = \mathcal{P}_\varepsilon(\mathbf{v} + \Delta \mathbf{v}_i)$. The projector operator \mathcal{P}_ε controls the criteria $\|\mathbf{v}\|_p \leq \varepsilon$. For example, for $p = \infty$:

$$\mathcal{P}_\varepsilon(\mathbf{v}) = \text{Clip}(\mathbf{v}, -\varepsilon, \varepsilon) \quad (16)$$

To improve the quality of k UAP the iterative procedure over X needs to be repeated several times until the desired universal fooling rate $(1-\delta)$ is reached, as in [26] (see Algorithm 2). The universal fooling rate for Top- k prediction is similar to Equation (18), except that \mathbf{v} does not depend on \mathbf{x} :

$$\text{UFR}_k[X] = \frac{1}{N} \sum_{i=1}^N \mathbf{1}_{\arg \max F(\mathbf{x}_i) \notin \arg \text{sort} F_i(\mathbf{x}_i + \mathbf{v})[k]} \quad (17)$$

Algorithm 2 k UAP

INPUT: k , ℓ_p -bound ε , fooling rate δ , dataset $X = \{\mathbf{x}_1, \dots, \mathbf{x}_N\}$, classifier F

- 1: $\mathbf{v} \leftarrow \mathbf{0}$
- 2: **while** $\text{UFR}_k[X] \leq 1 - \delta$ **do**
- 3: **for** $\mathbf{x}_i \in X$ **do**:
- 4: **if** $\arg \max F(\mathbf{x}_i) \in \arg \text{sort}(F(\mathbf{x}_i + \mathbf{v}))[k]$
- 5: **then**:
- 6: $\Delta \mathbf{v}_i = k\text{Fool}(k, \mathbf{x}_i + \mathbf{v}, F) \triangleright$ Algorithm 1
- 7: $\mathbf{v} \leftarrow \mathcal{P}_\varepsilon(\mathbf{v} + \Delta \mathbf{v}_i)$
- 8: **end if**
- 9: **end for**
- 10: **end while**

OUTPUT: Top- k Universal Adversarial Perturbation \mathbf{v}

5. Experiments

5.1. Experiments with k Fool

Here, we experimentally show the effectiveness and efficiency of k Fool algorithm. Different values of k lead to different presentation of the perturbations. In the experiments below we present results for a fixed k , however, the numerical results for other values of k are always similar (see Table 1).

For the experiments below we use following neural network architectures: LeNet [24] for MNIST test dataset, ResNet-20 [17] for CIFAR-10 test dataset and ResNet-18 [17] for ILSVRC2012 [11] validation dataset. To show the effectiveness of k Fool ($k = 3; 5$ for MNIST and CIFAR10, $k = 5; 10; 15; 20$ for ILSVRC2012, for other values of k we got similar results), we compare the Top- k fooling rate with DeepFool [27] and FGSM [14] (90% Top-1 fooling rate). Results shown in Table 1 illustrate that k Fool is indeed effective in terms of Top- k fooling rate. The metric to compare fooling rates is:

$$\text{FR}_k[X] = \frac{1}{N} \sum_{i=1}^N \mathbf{1}_{\arg \max F(\mathbf{x}_i) \notin \arg \text{sort} F_i(\mathbf{x}_i + \mathbf{v}(\mathbf{x}_i))[k]} \quad (18)$$

Figure 3 illustrates examples of a k Fool adversarial perturbation for $k = 5$, DeepFool [27] perturbation, and FGSM [14] perturbation. It can be observed that k Fool produces a hardly perceptible adversarial noise of a small norm. To quantitatively measure the efficiency (smallness) of k Fool perturbations, we compare it to existing techniques of generating adversarial examples: FGSM [14] and DeepFool [27]. Following [27], the numerical metric (the lesser - the better) to compare norms of adversarial perturbations for a dataset \mathcal{D} is:

$$\rho_p = \frac{1}{|\mathcal{D}|} \sum_{\mathbf{x} \in \mathcal{D}} \frac{\|\mathbf{r}(\mathbf{x})\|_p}{\|\mathbf{x}\|_p} \quad (19)$$

	DF [27]	FGSM [14]	k Fool $k=3$	k Fool $k=5$		DF [27]	FGSM [14]	k Fool $k=3$	k Fool $k=5$		DF [27]	FGSM [14]	k Fool $k=5$	k Fool $k=10$	k Fool $k=15$	k Fool $k=20$
FR_1	1.0	0.9009	1.0	1.0	FR_1	1.0	0.8919	1.0	1.0	FR_1	1.0	0.892	1.0	1.0	1.0	1.0
FR_2	0.0	0.4299	0.9994	0.9998	FR_2	0.0	0.7851	0.9972	0.9999	FR_5	0.0	0.538	0.995	0.998	1.0	1.0
FR_3	0.0	0.2206	0.9988	0.9994	FR_3	0.0	0.6615	0.9941	0.998	FR_{10}	0.0	0.428	0.062	0.998	0.997	0.999
FR_4	0.0	0.1181	0.2819	0.9987	FR_4	0.0	0.5348	0.1928	0.9962	FR_{15}	0.0	0.366	0.007	0.201	0.996	0.997
FR_5	0.0	0.0620	0.0935	0.9984	FR_5	0.0	0.4367	0.0502	0.9958	FR_{20}	0.0	0.328	0.0	0.053	0.301	0.996

(a) MNIST (LeNet)

(b) CIFAR10 (ResNet-20)

(c) ILSVRC2012 (ResNet-18)

Table 1. Comparison of fooling rates (Eq. (18)) of DF (DeepFool) [27], FGSM [14], and k Fool (ours) for different datasets and architectures.

	Metric	k Fool (ℓ_∞)	DF (ℓ_∞)	FGSM (90%)
MNIST	ρ_2	0.6659	0.3277	0.5598
	ρ_∞	0.2456	0.1116	0.1836
CIFAR10	ρ_2	0.0279	0.0122	0.3536
	ρ_∞	0.0165	0.0061	0.1533
ILSVRC2012	ρ_2	0.0061	0.0024	0.0095
	ρ_∞	0.0033	0.0012	0.0042

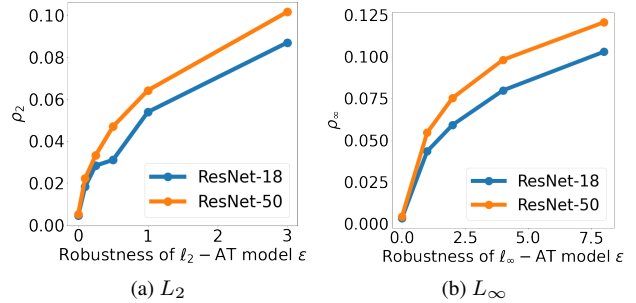
Table 2. Comparison of average relative ℓ_p -norms (Eq. (19)) of adversarial perturbations by k Fool ($k = 3$ for MNIST and CIFAR10, $k = 5$ for ILSVRC2012), FGSM [14] and DeepFool [27] algorithms.

Since FGSM [14] targets the ℓ_∞ -bounded perturbation, we use the ℓ_∞ version of DeepFool and k Fool for fair comparison (see Table 2). In the case of DeepFool and k Fool we reach our desired fooling condition (either Top-1 or Top- k) for 100% of images, however for FGSM increasing ε even to very large values, we cannot reach 100% fooling rate. For this reason, we use such values of ε for FGSM, that guarantee the fooling for some specific number of images (90% Top-1 fooling rate).

Based to the quantitative results in Table 2, it can be seen that k Fool generates very efficient perturbation both in terms of ℓ_2 and ℓ_∞ norms. k Fool either reaches the same average relative norms (ρ_p , Eq. (19)) as FGSM, or outperforms it, and has average relative norms comparable to DeepFool, however the goal of k Fool is more challenging, as it targets to perturb input data point such that true class is outside of Top- k prediction.

We also show the efficiency of k Fool in terms of running time. We compared k Fool to Top- k PGD attack, which is extension of PGD [22, 25] and Top- k CW [38] attack [38], which is extension of CW [8], for CIFAR-10 ($k = 3$) and Imagenet ($k = 5$). PGD [22, 25] and CW [8] are known to find minimal Top-1 perturbations. To extend PGD to Top- k scenario, we maximize losses of Top- k classes other than the true. As we see in Table 3, k Fool 60 times quickly finds Top- k adversarial perturbation compared to

	Top- k CW [38]	Top- k PGD	k Fool
Time (CIFAR-10)	30.4s	0.6s	0.5s
Time (ILSVRC2012)	33.3s	0.68s	0.68s
FR (CIFAR-10)	0.994	0.5	0.9941
FR (ILSVRC2012)	0.999	0.99	0.9984
ρ_2 (CIFAR-10)	0.0094	0.1	0.017
ρ_2 (ILSVRC2012)	0.0022	0.07	0.0043

Table 3. Comparison of sample processing time, fooling rate, ℓ_2 norms of k Fool, Top- k CW [38], and Top- k PGD for CIFAR-10 ($k = 3$) and ILSVRC2012 ($k = 5$).Figure 5. Average relative norms of k Fool ($k = 5$) of adversarially trained models over ILSVRC2012 validation dataset

Top- k CW [38] for CIFAR-10, and 42 times more quickly for ILSVRC2012, though Top- k CW finds perturbation of lesser norm.

Adversarial training (AT) [14, 25] has been recently proposed as an empirical defense to make models robust to Top-1 adversarial perturbations. AT models are trained on Top-1 PGD adversarial examples instead of clean samples. This models have been shown to be prone to Top-1 adversarial perturbations, however, it is interesting how adversarial training affects norms of Top- k perturbations. To explore this, we tested k Fool on AT-models (pretrained from [31]) trained at different robustness strengths ε . The results are shown in Figure 5. As we see from the plots, adversarial training helps to resist not only Top-1 perturbations, but also for Top- k perturbations.



Figure 6. Examples of perturbed images with a single quasi imperceptible Top- k Universal Adversarial Perturbation generated for MobileNetV2 and $k = 3$. Under each image the wrong Top-3 prediction is shown, when the perturbation is added.

Classifier	Metric	UAP	k UAP ($k = 3$)
ResNet-18	Top-1	0.7725	0.7789
	Top-2	0.7015	0.7109
	Top-3	0.6598	0.6720
VGG-16	Top-1	0.7909	0.8231
	Top-2	0.7265	0.7661
	Top-3	0.6882	0.7320
MobileNetV2	Top-1	0.8851	0.9154
	Top-2	0.8373	0.8791
	Top-3	0.8033	0.8550

Table 4. Universal fooling rates (Eq. (17)) of different architectures

	ResNet-18	VGG-16	MobileNetV2
ResNet-18	0.6720	0.2688	0.3040
VGG-16	0.3448	0.7320	0.4211
MobileNetV2-18	0.2465	0.1500	0.8550

Table 5. Cross-network transferability of k UAPs ($k = 3$). The rows indicate the network for which the k UAP is computed, and the columns indicate the network for which the fooling rate is reported.

5.2. Experiments with k UAP

For our experiments with ILSVRC2012 [11] dataset we used the following pre-trained architectures: VGG-16 [34], ResNet-18 [17], MobileNetV2 [32].

To generate Top- k universal adversarial perturbation we use 10000 images from validation set of ILSVRC2012 [11] dataset, such that each of 1000 classes are represented by 10 samples, as the train set. The remaining 40000 images from ILSVRC2012 validation set is used as the test set. We constraint the universal perturbation \mathbf{v} by ℓ_∞ norm bounded by $\varepsilon = 10$, which is significantly smaller than the average ℓ_∞ norm of the validation set: $\frac{1}{|\mathcal{D}|} \sum_{\mathbf{x} \in \mathcal{D}} \|\mathbf{x}\|_\infty \approx 250$. These

criteria produces quasi-imperceptible Top- k Universal Adversarial Perturbations. Examples of such perturbed images

from test set are shown in Fig. 6. In Fig. 6 one single Top-3 universal adversarial perturbation, generated using k UAP algorithm for MobileNetV2 [32] architecture, was added to natural images.

We also generate Top- k Universal Adversarial Perturbations using k UAP for different deep neural networks. Fig. 7 shows generated k UAPs ($k = 3$) corresponding to ResNet-18 [17], VGG-16 [34], MobilenetV2 [32] for ILSVRC2012 dataset. Similarly to [26], these perturbations contain visually structured patterns, which might reveal some interesting information about DNNs. We report their fooling rates on test set and compare to UAP in Table 4. Even UAP’s target is not Top- k prediction, it shows good fooling rate, however k UAP outperforms.

It is well-known that the UAPs [26] have property to transfer across networks, which make them ‘doubly-universal’. It is interesting to check if proposed k UAPs are also transferable. It is expected that they are more network-specific, which is indeed confirmed by Table 5, however, the constructed perturbations give fooling rate sufficiently higher than random perturbation.

It should be mentioned that Top- k Universal Adversarial Perturbations shown in Fig. 7 are not unique perturbations and there are a numerous perturbations satisfying above criteria. The diversity for example might be reached by changing the training batch of images, however, it is interesting to see how fooling rate depends on the size of training set.

To explore that we select 1, 2, 3, 4 samples from each class from previous training set (10000 images) which corresponds to 1000, 2000, 3000, 4000 size values and construct universal perturbation using UAP [26] and our proposed k UAP ($k = 3$). We test all perturbations on the same test set of 40000 images that was used before. Figure 8 demonstrates the Top-3 fooling rate for UAP and k UAP using different sizes of training set. As it can be seen, k UAP generates much stronger Top- k universal adversarial perturbations than UAP [26] for the same size of training dataset.

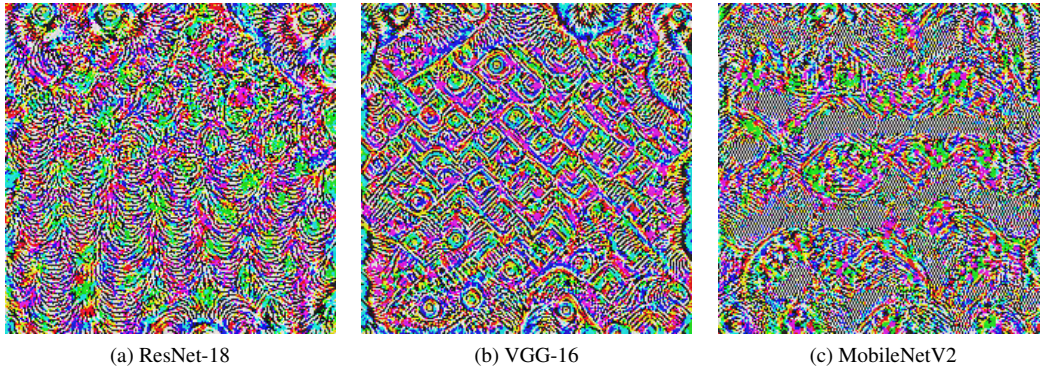


Figure 7. Result of k UAP ($k = 3$) to different deep neural networks for ILSVRC2012

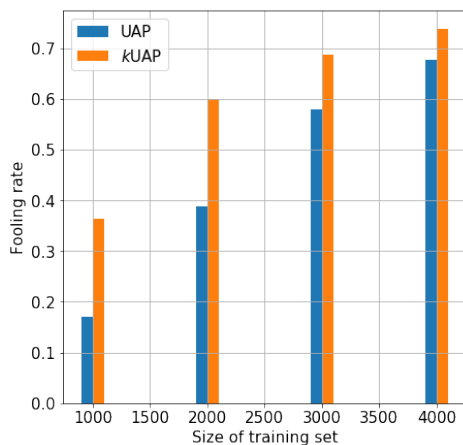


Figure 8. The test set fooling rate on the size of training set

6. Related Work

In the task of image classification, class ambiguity is a common problem especially when the number of classes increases. Thus, it makes sense to allow making k guesses and it motivates to evaluate classifiers based on the Top- k error, instead of the typical Top-1 error. This problem is computationally easier to solve (scales better), and produces the better accuracy score. Several Top- k losses were suggested recently to yield the better Top- k accuracy score [23, 6, 13, 10].

Initially found in [35], adversarial examples have gained significant attention. Goodfellow et.al [14] first proposed a single-step way of constructing adversarial perturbations, and its iterative extension was proposed in [22]. DeepFool [27] is an efficient geometric approach of finding very small adversarial perturbations. After it was shown in [26] that, using DeepFool, it is possible to construct UAPs, several other methods were proposed [20, 37, 29, 28, 16]. In [29, 28], it was proposed to craft data-free UAPs, using different objectives. In [20], it was proposed to use (p, q) -singular vectors to craft UAPs with a few data sam-

ples. In [37], it was proposed to attack images with UAPs in a black-box manner, using Fourier basis. In [16], generative models were used to construct UAPs. UAPs is not the problem in the image classification task only and were generalized to semantic segmentation [18], text classification [5], speech recognition [30] and audio classification [1]. Recently, Jia et al. [19] provided tight bounds of certified robustness for a Top- k adversarial perturbation in ℓ_2 norm, however existing adversarial perturbations are mostly concerned only with Top-1 prediction. In [38] ordered Top- k attack was suggested, however, their method relies on C&W attack [8], which is not an efficient way of constructing adversarial perturbation, as requires a lot of time. To the best of our knowledge, no prior method of efficient constructing Top- k adversarial examples and Top- k UAPs was proposed.

7. Conclusion

In this work, we made step towards geometric understanding of decision boundaries of deep classifiers. We proposed an efficient geometry-inspired way of constructing Top- k adversarial perturbations and Top- k universal adversarial perturbations. We found our method as an efficient and effective technique. Our method k Fool outperforms existing techniques in Top- k fooling rate and finds Top- k adversarial perturbations of small norm. Based, on our proposed algorithm k Fool, we propose k UAPs: single perturbations mere addition of which to most of images pushes away correct outside of Top- k prediction. Our method k UAP outperforms UAP both in Top-1 and Top- k fooling rates.

The 'bisector' direction that simultaneously brings closer several decision boundaries has interesting interpretation. It normalizes the vectors towards each boundary and sums them up. Similar approaches can be helpful in multi-task learning, when the goal is to solve several tasks simultaneously.

References

- [1] Sajjad Abdoli, Luiz G Hafemann, Jerome Rony, Ismail Ben Ayed, Patrick Cardinal, and Alessandro L Koerich. Universal adversarial audio perturbations. *arXiv preprint arXiv:1908.03173*, 2019. 8
- [2] Moustafa Alzantot, Bharathan Balaji, and Mani Srivastava. Did you hear that? adversarial examples against automatic speech recognition. *arXiv preprint arXiv:1801.00554*, 2018. 1
- [3] Anish Athalye, Nicholas Carlini, and David Wagner. Obfuscated gradients give a false sense of security: Circumventing defenses to adversarial examples. *arXiv preprint arXiv:1802.00420*, 2018. 1
- [4] Anish Athalye, Logan Engstrom, Andrew Ilyas, and Kevin Kwok. Synthesizing robust adversarial examples. In *International conference on machine learning*, pages 284–293. PMLR, 2018. 1
- [5] Melika Behjati, Seyed-Mohsen Moosavi-Dezfooli, Mahdih Soleymani Baghshah, and Pascal Frossard. Universal adversarial attacks on text classifiers. In *ICASSP 2019-2019 IEEE International Conference on Acoustics, Speech and Signal Processing (ICASSP)*, pages 7345–7349. IEEE, 2019. 8
- [6] Leonard Berrada, Andrew Zisserman, and M Pawan Kumar. Smooth loss functions for deep top-k classification. *arXiv preprint arXiv:1802.07595*, 2018. 8
- [7] Tom B Brown, Dandelion Mané, Aurko Roy, Martín Abadi, and Justin Gilmer. Adversarial patch. *arXiv preprint arXiv:1712.09665*, 2017. 1
- [8] Nicholas Carlini and David Wagner. Towards evaluating the robustness of neural networks. In *2017 IEEE Symposium on Security and Privacy (SP)*, pages 39–57. IEEE, 2017. 1, 6, 8
- [9] Nicholas Carlini and David Wagner. Audio adversarial examples: Targeted attacks on speech-to-text. In *2018 IEEE Security and Privacy Workshops (SPW)*, pages 1–7. IEEE, 2018. 1
- [10] Xiaojun Chang, Yao-Liang Yu, and Yi Yang. Robust top-k multiclass svm for visual category recognition. In *Proceedings of the 23rd ACM SIGKDD International Conference on Knowledge Discovery and Data Mining*, pages 75–83, 2017. 8
- [11] Jia Deng, Alex Berg, Sanjeev Satheesh, H Su, Aditya Khosla, and L Fei-Fei. Imagenet large scale visual recognition competition 2012 (ilsvrc2012). See *net.org/challenges/LSVRC*, page 41, 2012. 5, 7
- [12] Kevin Eykholt, Ivan Evtimov, Earlene Fernandes, Bo Li, Amir Rahmati, Chaowei Xiao, Atul Prakash, Tadayoshi Kohno, and Dawn Song. Robust physical-world attacks on deep learning visual classification. In *Proceedings of the IEEE Conference on Computer Vision and Pattern Recognition*, pages 1625–1634, 2018. 1
- [13] Yanbo Fan, Siwei Lyu, Yiming Ying, and Baogang Hu. Learning with average top-k loss. In *Advances in neural information processing systems*, pages 497–505, 2017. 8
- [14] Ian J Goodfellow, Jonathon Shlens, and Christian Szegedy. Explaining and harnessing adversarial examples. *arXiv preprint arXiv:1412.6572*, 2014. 1, 2, 4, 5, 6, 8
- [15] Tianyu Gu, Brendan Dolan-Gavitt, and Siddharth Garg. Bad-nets: Identifying vulnerabilities in the machine learning model supply chain. *arXiv preprint arXiv:1708.06733*, 2017. 1
- [16] Jamie Hayes and George Danezis. Learning universal adversarial perturbations with generative models. In *2018 IEEE Security and Privacy Workshops (SPW)*, pages 43–49. IEEE, 2018. 8
- [17] Kaiming He, Xiangyu Zhang, Shaoqing Ren, and Jian Sun. Deep residual learning for image recognition. In *Proceedings of the IEEE conference on computer vision and pattern recognition*, pages 770–778, 2016. 5, 7
- [18] Jan Hendrik Metzen, Mummadi Chaithanya Kumar, Thomas Brox, and Volker Fischer. Universal adversarial perturbations against semantic image segmentation. In *Proceedings of the IEEE International Conference on Computer Vision*, pages 2755–2764, 2017. 8
- [19] Jinyuan Jia, Xiaoyu Cao, Binghui Wang, and Neil Zhenqiang Gong. Certified robustness for top-k predictions against adversarial perturbations via randomized smoothing. *arXiv preprint arXiv:1912.09899*, 2019. 8
- [20] Valentin Khruikov and Ivan Oseledets. Art of singular vectors and universal adversarial perturbations. In *Proceedings of the IEEE Conference on Computer Vision and Pattern Recognition*, pages 8562–8570, 2018. 8
- [21] Stepan Komkov and Aleksandr Petiushko. Advhat: Real-world adversarial attack on arcface face id system. *arXiv preprint arXiv:1908.08705*, 2019. 1
- [22] Alexey Kurakin, Ian Goodfellow, and Samy Bengio. Adversarial examples in the physical world. *arXiv preprint arXiv:1607.02533*, 2016. 2, 6, 8
- [23] Maksim Lapin, Matthias Hein, and Bernt Schiele. Loss functions for top-k error: Analysis and insights. In *Proceedings of the IEEE Conference on Computer Vision and Pattern Recognition*, pages 1468–1477, 2016. 8
- [24] Yann LeCun, Léon Bottou, Yoshua Bengio, and Patrick Haffner. Gradient-based learning applied to document recognition. *Proceedings of the IEEE*, 86(11):2278–2324, 1998. 5
- [25] Aleksander Madry, Aleksandar Makelov, Ludwig Schmidt, Dimitris Tsipras, and Adrian Vladu. Towards deep learning models resistant to adversarial attacks. *arXiv preprint arXiv:1706.06083*, 2017. 6
- [26] Seyed-Mohsen Moosavi-Dezfooli, Alhussein Fawzi, Omar Fawzi, and Pascal Frossard. Universal adversarial perturbations. In *Proceedings of the IEEE conference on computer vision and pattern recognition*, pages 1765–1773, 2017. 1, 4, 5, 7, 8
- [27] Seyed-Mohsen Moosavi-Dezfooli, Alhussein Fawzi, and Pascal Frossard. Deepfool: a simple and accurate method to fool deep neural networks. In *Proceedings of the IEEE conference on computer vision and pattern recognition*, pages 2574–2582, 2016. 1, 2, 4, 5, 6, 8
- [28] Konda Reddy Mopuri, Aditya Ganeshan, and R Venkatesh Babu. Generalizable data-free objective for crafting universal adversarial perturbations. *IEEE transactions on pattern analysis and machine intelligence*, 41(10):2452–2465, 2018. 8

- [29] Konda Reddy Mopuri, Utsav Garg, and R Venkatesh Babu. Fast feature fool: A data independent approach to universal adversarial perturbations. *arXiv preprint arXiv:1707.05572*, 2017. 8
- [30] Paarth Neekhara, Shehzeen Hussain, Prakhar Pandey, Shlomo Dubnov, Julian McAuley, and Farinaz Koushanfar. Universal adversarial perturbations for speech recognition systems. *arXiv preprint arXiv:1905.03828*, 2019. 8
- [31] Hadi Salman, Andrew Ilyas, Logan Engstrom, Ashish Kapoor, and Aleksander Madry. Do adversarially robust imagenet models transfer better? In *ArXiv preprint arXiv:2007.08489*, 2020. 6
- [32] Mark Sandler, Andrew Howard, Menglong Zhu, Andrey Zhmoginov, and Liang-Chieh Chen. Mobilenetv2: Inverted residuals and linear bottlenecks. In *Proceedings of the IEEE conference on computer vision and pattern recognition*, pages 4510–4520, 2018. 7
- [33] Mahmood Sharif, Sruti Bhagavatula, Lujio Bauer, and Michael K Reiter. Accessorize to a crime: Real and stealthy attacks on state-of-the-art face recognition. In *Proceedings of the 2016 acm sigsac conference on computer and communications security*, pages 1528–1540, 2016. 1
- [34] Karen Simonyan and Andrew Zisserman. Very deep convolutional networks for large-scale image recognition. *arXiv preprint arXiv:1409.1556*, 2014. 2, 7
- [35] Christian Szegedy, Wojciech Zaremba, Ilya Sutskever, Joan Bruna, Dumitru Erhan, Ian Goodfellow, and Rob Fergus. Intriguing properties of neural networks. *arXiv preprint arXiv:1312.6199*, 2013. 1, 2, 8
- [36] Florian Tramer, Nicholas Carlini, Wieland Brendel, and Aleksander Madry. On adaptive attacks to adversarial example defenses. *arXiv preprint arXiv:2002.08347*, 2020. 1
- [37] Yusuke Tsuzuku and Issei Sato. On the structural sensitivity of deep convolutional networks to the directions of fourier basis functions. In *Proceedings of the IEEE Conference on Computer Vision and Pattern Recognition*, pages 51–60, 2019. 8
- [38] Zekun Zhang and Tianfu Wu. Adversarial distillation for ordered top-k attacks. *arXiv preprint arXiv:1905.10695*, 2019. 6, 8